Original Articles

A Novel Method for Quantifying Shape Deformation Applied to Biocompatibility Testing

VOLKER METZLER,* HANS BIENERT,† THOMAS LEHMANN,* KHOSROW MOTTAGHY,‡ AND KLAUS SPITZER*

Cytotoxicity tests are important for the screening and evaluation of biocompatibility of artificial organs. Morphologic changes of cells that were contacted biomaterials or biomaterial extracts indicate their toxicity. However, information on cytotoxic effects is still obtained by subjective visual inspection of microscopic samples. In this article, a novel computer assisted method is introduced. The automatic analysis of digitized micrographs is achieved in several stages: segmentation, separation, classification, and measurement. The segmentation of the image is provided by a new local adaptive thresholding technique, which adapts the threshold window sizes onto local gray level distribution and yields optimal window sizes. The actual threshold is obtained by maximizing interclass variances and minimizing intraclass variance. For the separation of connected cells, the binarized samples are cleaned from "false" markers by morphologic filtering. The subsequent separation is a two phase approach. Information levels are generated top-down by successively applying an enhanced erosion operator, which yields markers and filters noise usually evolving from multiple erosions. The converse bottom-up integration of the eroded markers is performed by successively applying an enhanced dilation operator, which reconstructs the cells and prevents merging of already separated objects. The subsequent measuring provides quantitative parameters of the distribution of size and compactness of the cells contained within the sample. The method was evaluated by L-929 fibroblasts that were in contact with 0%, 5%, and 10% concentrations of ethanol. For each concentration, 268 images of the cell populations were captured. The obtained quantitative parameters are highly correlated to the common verbal description of morphologic changes. Therefore, the proposed automatic method has several advantages compared with subjective examinations. The results allow an objective comparison of the quantification of phenomena; the subjective influence of the observer is eliminated; and the laboratory staff is relieved of time consuming routine work.
***ASAIO Journal* 1999; 45:264–271.**

The most important presupposition for the development of medical devices is the biocompatibility of the used materials. According to Gurland *et al.*,[1] biocompatibility is defined as the ability of a material, device, or system to perform without clinically significant host response in a specific application.

A comprehensive understanding of biocompatibility includes the determination of different parameters like cytotoxicity, mutagenicity, carcinogenicity, hemocompatibility, sensitization, and irritation. Even though cytotoxicity is only one aspect of biocompatibility, cytotoxicity studies are appropriate for screening and evaluation of biocompatibility of new or modified materials to be used for medical devices. Until now, cytotoxicity studies have been limited to qualitative or semiquantitative analysis using established, transformed, or neoplastic cell lines. The progress achieved in the last few years associated with the culture of mammalian cells enabled scientists to develop quantitative assays for cytotoxicity assessments that are highly reproducible and sensitive.[2,3] Endpoints that provide information about cellular function or cellular compartments are indicative of cytotoxicity. Examples are structural integrity of the cell, functioning of the mitochondria, and DNA synthesis. Different techniques, such as scanning electron microscopy, flow cytometry, MTT/XTT tests, BrdU-incorporation, and dye exclusion assays have been used to determine these parameters.

The use of cell cultures for toxicity testing of medical devices and their biomaterials is covered by ISO10993/EN30993. Part 5 describes the basic requirements for cell culture techniques.[4] The microscopic examination of cell cultures to evaluate morphologic changes is most frequently used in cytotoxicity evaluation of biomaterials. Usually, this is related to subsequent interactive measurement of relevant features. After appropriate staining and microscopy, even minor alterations in the cell morphology of cultured cells exposed to a chemical or biomaterial become observable. The morphologic changes indicate toxicity and can be related to pathologic effects caused by the biomaterial. Toxic substances eluted from foreign surfaces interact at the cellular level with cell membranes, cell organelles, protein synthesis, DNA synthesis, and cell division. These substances arise from additives, process contaminants and residues, leachable substances, and biodegradation products.

Ethanol in low concentrations is a well known toxin for hepatocytes, osteoblasts, fibroblasts, Kupffer cells, and other cell lines. The cytotoxic effects depend on the exposure time and the concentration of ethanol. The differences in ethanol tolerance among cell lines are very low.[5] Ethanol affects several metabolic and mitotic processes in cultured cells. Examples are cell membrane alterations,[6,7] the disturbance of the intracellular signal transduction process,[8] cell proliferation,[9]

From the *Institute of Medical Informatics, Aachen University of Technology (RWTH); †Interdisciplinary Center for Clinical Research on Biomaterials, Aachen University of Technology (RWTH); ‡Institute of Physiology, Aachen University of Technology (RWTH), Aachen, Germany.

Submitted for consideration June 1998; accepted for publication in revised form November 1998.

Reprint requests: Dipl.-Inform. Volker Metzler, Institut für Signalverarbeitung und Proze, TZL, Seelandstr. 1a, Medizinische Universität Lübeck, D-23569 Lübeck, Germany.

and a decrease of cytoskeletal proteins.[10] In all these cases, ethanol provides a reproducible cytotoxic response.

Assessment of cell morphology is, if performed by an experienced scientist, a reliable method. By development of a computer assisted method, we expect to gain more objective and standardized results. The quantitative method is to be used only for material extracts.

Changes in morphology are the general endpoint of cellular toxicity, which are often secondary effects. Toxic effects on cells may result in overall changes in cell shape or minor changes in cellular structures. One type of general structural change is the rounding up and shrinking of cells that normally are extended and have differentiated contours.[11,12] The shape of cells is ultimately determined by the structure and composition of the intracellular cytoskeletal elements. Changes of cell shapes in response to toxic effects of foreign surfaces reflect toxin induced rearrangements of the cytoskeleton. These toxins affecting cytoskeletal components may also inhibit cellular movements and filament-dependent uptake or release of particles.

Naturally, the evaluation of cytotoxicity by means of microscopic observation of cell deformation is qualitative. Therefore, the effects can only be recorded descriptively as deviation from normal morphology. This causes the well known ambiguities in interpretation and comparison of results. The acquisition of reproducible morphologic cytotoxicity data of biomaterial extracts is certainly feasible with the use of computer assisted methods that evaluate cell populations automatically and quantitatively. The use of those algorithms in biomedical image analysis became practical in the past decades because of the enormous use in the computational power of modern image processing systems. This technical development, combined with advanced staining techniques from molecular biology, result in computer assisted examination of relevant image features in microscopic samples.[13] In digital image processing, the structural analysis of cell populations is often performed by methods of mathematical morphology.[14] Morphologic filters play a major role in microscopic image interpretation because of their object-, rather than frequency-oriented operations. This versatile theory can be used at different stages of the automated feature quantification process, the preprocessing,[15] the segmentation,[16] or the feature extraction.[17]

However, these benefits from modern technologies have not been established in clinical routine. For example, the deformation of the natural shape of Hemalaun-stained L-929 cells exposed to ethanol is still determined by visual inspection.

In this paper, cytotoxicity determination is supported by a novel computerized method for geometric shape analysis of cells extracted from digitized samples. The aim is to measure quantitative and discriminative parameters. For this purpose, segmentation, separation, classification, and quantification of cells is performed using specially designed image processing algorithms. Image segmentation is one of the most important steps.

Because of the numerous problems that arise from variances in illumination, layer thickness, or staining concentration,[18,19] only a few of the proposed segmentation techniques are applicable to digital cytologic imaging.[20,21] Therefore, a local adaptive thresholding technique was specially developed to cope with problems related to cytologic samples (described in "Segmentation of the Digital Samples").

Special algorithms have been designed and applied to the geometric separation and classification of binary objects to quantify their shapes. This is achieved by cascaded application of morphologic filters (described in "Separation and Classification by Mathematical Morphology"). To determine cytotoxicity, we extract quantitative parameters such as size, perimeter, compactness, and the center of gravity of the scatter diagram (described in "Quantification of Shape Parameters"). The significance of the parameters extracted by our algorithm is experimentally verified. Fibroblasts were destroyed by defined concentrations of ethanol and acquired using digital microscopy (described in the "Materials and Methods" section). The changes in shape are determined by our novel algorithm for automatic shape analysis. The results of this evaluation are presented in the "Results" section and discussed in greater detail in the "Discussion" section.

Algorithm for Automatic Shape Analysis

After staining, preparation, and digital acquisition of cytologic samples, the extraction of quantitative parameters is always performed by the following steps:

Segmentation. Image segmentation results in relevant and nonrelevant connected regions (e.g., object and background). This includes preprocessing steps such as object dependent noise filtering and contrast enhancement.

Separation and Classification. The regions obtained by any segmentation process do not correspond exactly with the objects in the image. Some regions might contain more than one object (undersegmentation), whereas others represent less than one object (oversegmentation). The separation and classification step can be viewed as a postprocessing of segmentation, preparing the image for the subsequent measurements. In the special case of shape analysis of monolayered cell populations, this step performs the separation of agglomerated cells into single countable and measurable segments. In addition, distorted cells are detected (classification) and removed.

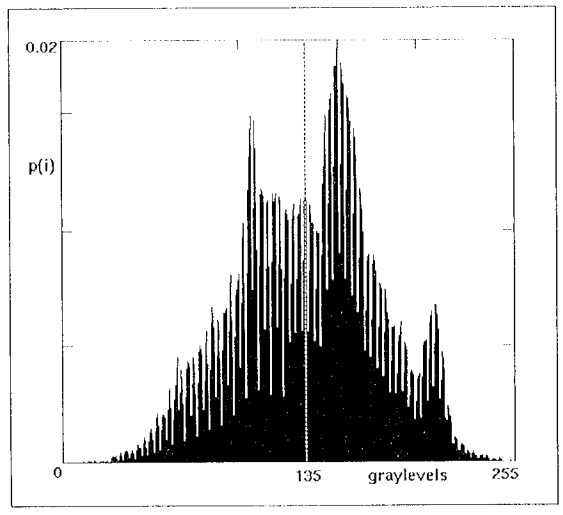

Figure 1. The *a priori* probability $p(i)$ for all gray levels i of a micrograph (Figure 2a) is visualized in the histogram. The given global threshold was used to generate Figure 2b.

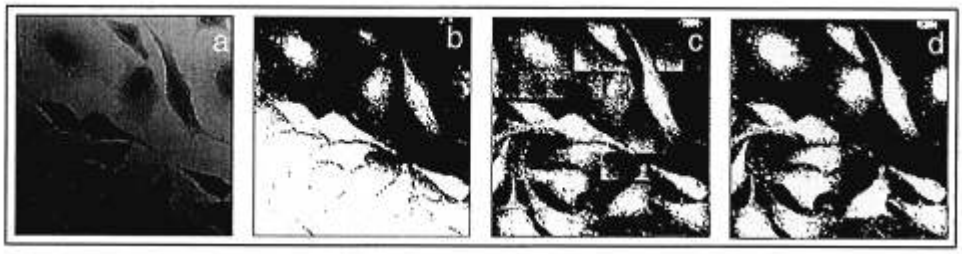

Figure 2. The cytological sample shows connected and inhomogeneously distributed cells (a). A global histogram thresholding technique is used in *b*. The binarization (c) is obtained by local thresholds of constant window size, whereas *d* results from local adaptive window sizes.

Measurement. Quantitative parameters are measured from the image material. They describe discriminative features, which allow the determination of the toxicity of the material that was in contact with the cells.

Segmentation of the Digital Samples

After contrast enhancement and noise reduction, the image is partitioned into nonoverlapping regions corresponding to the interpretation of human observers. When the population consists of L-929 fibroblasts, this segmentation step should result in two regions: the cells and the image background. Therefore, it is obvious one can calculate a binarization of the image. In a binary image, any pixel contains either the gray level 0 (black/background) or 1 (white/object).

If all objects are of equal gray level characteristics (the cells are of the same type) a histogram thresholding technique can be applied. A histogram gives the one-dimensional *a priori* probability for all gray levels in the image (**Figure 1**). Usually, the gray levels occurring within the objects differ significantly from those in the background. This results in a bimodal histogram function that can be split into two parts by one global threshold.

However, in light micrographs from biologic samples usually both illumination and slice thickness may change significantly (**Figure 2a**). In addition, the concentration of staining cannot be assumed to be constant, which causes further problems for segmentation. Therefore, global histogram thresholding results in poor segmentation quality (**Figure 2b**). Improved results are obtained by local techniques, which determine independent thresholds for subimages (local windows) of constant size. However, if the distribution of objects in the image is not homogeneous, local approaches cause rectangular artifacts (**Figure 2c**).

Because large gray level variances require small window sizes, and vice versa, the threshold window sizes are adapted to the local gray level distributions. The window size is increased until the local variance meets the global variance, *i.e.*, the presence of different regions can be assumed. Generally, any kind of thresholding technique could be applied to decide whether the center pixel of the window belongs to the object or to the background. For segmentation of the L-929 populations, the histogram thresholding technique proposed by Otsu was chosen.[22] This technique yields the threshold with minimal interclass variance and maximal intraclass variance. The adaptive technique prevents the binarization errors of the static techniques (**Figure 2d**).

Separation and Classification by Mathematical Morphology

Because of detection errors and the image acquisition itself, the binarized images are noisy, and continuous cells might result in connected segments (**Figure 2d**). For subsequent quantification, noise filtering and the separation of the detected regions into single objects are required. This is performed by means of mathematical morphology, which provides powerful tools for the manipulation of binary objects.[14]

Because the magnification of the microscope and the expected minimal size of totally damaged fibroblasts are known, the classification of binary segments into cells and noise can easily be performed by morphologic reconstruction filters. The resulting binary objects are then separated into single cells by a cascaded approach.

Several deagglomeration algorithms are described in the

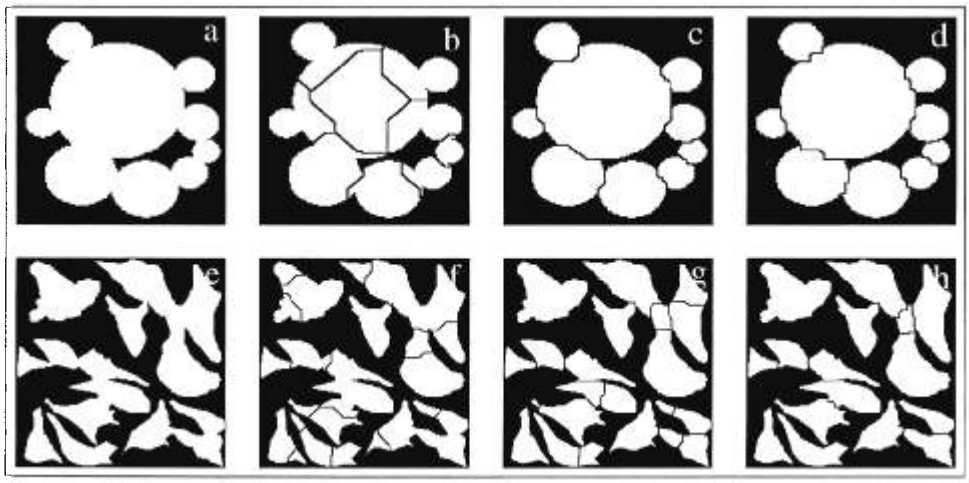

Figure 3. The synthetic images *a* and *e* show objects to be separated. The separations (b and f) were generated by a reconstruction from filtered ultimate eroded points, whereas *c* and *g* result from the reconstruction of filtered maxima of the distance transform. The cascaded separation algorithm yielded good results in both cases (d and h).

literature, *e.g.*, Serra's[23] algorithm is based on the ultimate eroded points of the image. The image is successively eroded until single pixels (markers) are obtained, each representing one single object. The separation lines between the segments are determined to have the maximal distance from all adjacent markers. Partitioning of the image is performed by overlaying the separation lines to the original image.

Figure 3 exemplifies Serra's[23] algorithm on both synthetic (**Figure 3a**) and natural (**Figure 3e**) materials. The separations shown in **Figure 3, b and f** were reconstructed from the filtered ultimate eroded points. The disadvantages are that all objects have to be of similar size and shape. Compact objects of different size lead to incorrect markers because the marker generation is size independent (**Figure 3b**). Moreover, objects with irregular shapes produce too many markers (**Figure 3f**), because the geometric interpretation is drawn from one single level.

Figure 3, c and g shows the separation results obtained by a reconstruction that starts with the maxima of the distance transform.[24] Although the distance transform is able to handle objects with different sizes (**Figure 3c**), the irregular shape of cells again causes oversegmentation (**Figure 3g**).

However, progressive segmentation using markers and applying complete object information afterward is a common concept in mathematical morphology.[16] In our algorithm, the separation of the agglomerated cells into single measurable fibroblasts is performed in two phases.

Marker Generation. A marker is just an indicator for the presence of an object but does not contain any shape information on the corresponding cell. The basic assumption is that two cells touching each other can be transformed into two separated markers by successive erosions. A number of marker levels are calculated by successive application of an *enhanced erosion operator*. The operator consists of a common erosion and a masked opening. These successive openings remove "false markers" that usually occur for multiple erosions of structured binary images. This prevents oversegmentation.

Reconstruction. The reconstruction of the original cells from their markers is achieved by successive application of an enhanced dilation operator. The markers of different marker levels are added level by level and dilated to the size and shape of the cell they represent. The merging of two separate markers is prevented by the operator. This way of reconstructing the markers yields sensible separations, even if the objects are different in size and shape.

Compared with the common separation techniques, our cascaded design avoids both drawbacks, size dependent markers and oversegmentation due to irregular shapes. The multilevel generation and filtering of markers is independent of the object size (**Figure 3d**), whereas their stepwise reconstruction according to the objects that they represent is not affected by the object's shape (**Figure 3h**).

Quantification of Shape Parameters

For the determination of exact parameters from digital images, two important points have to be considered: First, the transition from analog biologic objects to digital objects is crucial. Caused by the image sampling; theorems from Euclidean geometry do not hold in the discrete domain. Second, complex characteristic features of an object's morphology need to be expressed by single numbers, which have to discriminate between the different stages of morphologic changes and consequently for the toxicity of a biomaterial.

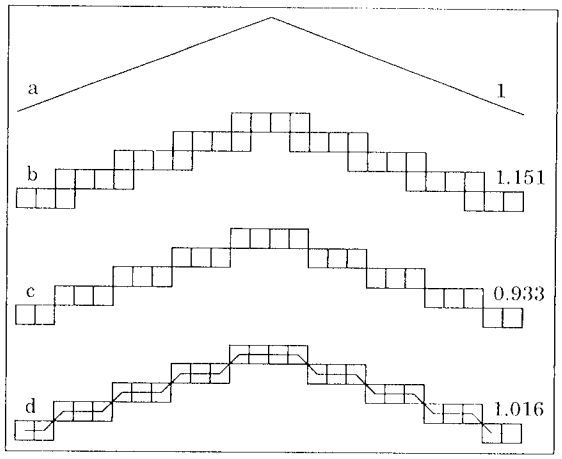

Figure 4. The lengths of the digitized line (a) can be measured in different ways. *b* is measured by a four-connected grid, *c* by an eight-connected grid, and *d* by an eight-connected grid with diagonal correction. The displayed lengths are normalized to that of the continuous line (a).

Measuring Continuous Objects in Digital Space. The digitization and binarization of a sample only yields an approximation of the continuous biologic objects. Because the charge–coupled–device (CCD) cameras used for image discretization are not related to the frequencies occurring within the images, it is obvious that the deviation between the lengths of continuous and digital contours decreases if the resolution of image capturing is increased.[25] Several methods have been proposed to measure the length of digital contours.[26] The most commonly used approaches are shown in **Figure 4**. Using a four-connected grid (**Figure 4b**), only horizontal and vertical steps are possible. The number of boundary pixels normalized by their absolute size results in an approximation of the length, which is usually larger than the continuous length. The use of an eight-connected grid (**Figure 4c**) improves the result because diagonal steps are allowed. However, the measured lengths are usually too small. The lowest deviation between digital and analogue lengths is obtained by an extension of the eight-connected grid, which corrects the diagonal steps to an adjacent pixel by the factor $\sqrt{2}$ (**Figure 4d**). The latter technique yields best results because the diagonal behavior is most realistic. The normalized lengths given in **Figure 4** show the described effect.

Quantification of Shape. The shape of objects is most important for the analysis of microscopic structures. Hence, it must be described exactly by a comprehensive measure. Different methods exist to quantitatively determine a complex feature such as shape.[25] Shape factors that are adapted to special cytologic problems are presented in Payne *et al.*[27] In fact, the representation of shape by a parameter requires enormous data compression, and there is no optimal parameter covering all aspects of shape interpretation.

The *aspect-ratio* is often used to quantify the elongation of binary objects because it uses indirect length measures. The aspect-ratio is obtained from length and width of the minimal bounding box:

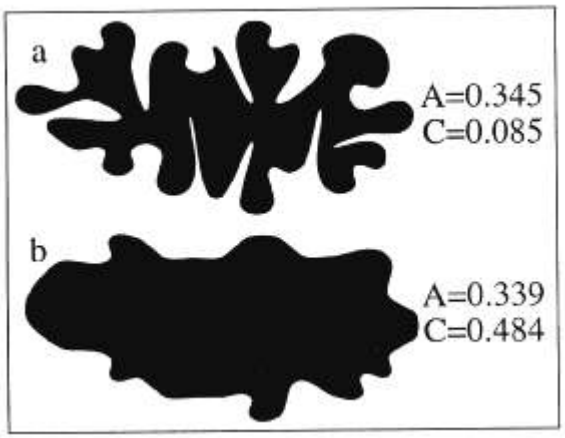

Figure 5. The shape of the two objects is obviously different. Parameters like the aspect-ratio *A* cannot be used to discriminate between the objects, because their spatial extent is similar. The compactness *C* yields discriminative values.

$$A = 1 + \frac{4}{\pi}\left(\frac{\text{length}}{\text{width}} - 1\right) \quad \text{with} \quad 0 \le A \le 1 \qquad (1)$$

The aspect-ratio requires additional computation to obtain rotation invariant measures. For example, each object is adjusted by a hotelling transform before the aspect-ratio is calculated. Additionally, the number of inflection points of the contour is not considered by such measures. Furthermore, the aspect-ratio is insensitive to irregularities of the shape (**Figure 5**).

To quantify cytotoxicity of cell populations, the shape irregularities are the most important characteristics to be measured. An appropriate parameter for this purpose is the *compactness*:

$$C = \frac{4\pi \cdot \text{area}}{\text{perimeter}^2} \quad \text{with} \quad 0 \le C \le 1 \qquad (2)$$

The compactness yields the ratio between area and perimeter of an object, which estimates the shape irregularities rather than the object's elongation. The compactness is rotation invariant, which reduces the computational overhead compared with the prior measure. **Figure 5** shows the properties of the two described parameters.

Materials and Methods

Mouse connective tissue fibroblasts (cell line L-929, DSM ACC 2, DSM, Braunschweig, Germany) were used to perform the quantitative image analysis. The L-929 cell line is the *de facto* standard for *in vitro* testing of biomaterials and is recommended in ISO10993 and EN30995 standards. The fibroblasts are grown in monolayers with a doubling time of approximately 24 hours. The L-929 cells were routinely cultured in tissue culture polystyrene flasks (Falcon, Heidelberg, Germany) at 37°C with 7.5% CO_2 and harvested after treatment with trypsin (0.25%, Gibco, Eggenstein-Leopoldshafen, Germany). The culture medium was 90% RPMI 1640 (Bio Whittacker, Vervier, Belgium) and 10% fetal calf Serum (Bio Whittacker, Vervier, Belgium). The cells were free of mycoplasma tested by the DAPI assay. Cells were counted with an electronic cell counter (Casy 1 Model TT, Schärfe Systems, Reutlingen, Germany).

For the experiments, silicone rubber blocks (Flexiperm-Mikro-12, Heraeus, Hanau, Germany) were mounted on slides. Each rubber block contains 12 holes, each with a diameter of 6 mm and a depth of 5 mm. Four slides were placed in a multiwell (Quadriperm, Heraeus, Germany). Cell suspension (100 μl) with a density of 30,000 cells/ml were placed in each cavity. The cells were incubated under specific culture conditions. After 24 hours the medium was discarded and replaced with test medium containing ethanol (ethanol concentrations used were 0, 5, 10, 15, 20, 25, 30, 40, and 50% v/v). The corresponding concentrations after 24 hours of incubation were 0, 3.35, 6.98, 10.25, 14.06, 16.95, 22.07, 26.56, and 34.53% v/v.

The cells were exposed to ethanol for 24 hours. After incubation the cells were gently rinsed with PBS, fixed in 3.5% formaldehyde for 10 minutes, stained with the basic dye haematoxylin (Merck, Darmstadt, Germany), and added to the cell specimens for 10 minutes. This treatment was followed by rinsing in water and resulted in a blue colored complex. This complex was positively charged and bound to negatively charged cell components.

The toxic effects on cells were evaluated quantitatively by assessing the general morphology, vacuolation, and shape of the nucleus by our novel geometric shape analysis. The cellular response was also recorded by direct morphologic observation with a DMR microscope (Leitz, Tübingen, Germany) at ×100 magnification. The observation was aligned with a series of digitized images (768 × 512 pixel matrix) acquired by a 3 chip CCD color camera (DXC–930P, Sony, Japan) and an imaging system, Quantimet 600C (Leica, Bensheim, Germany). The algorithms for automatic image analysis were designed on a UNIX platform using the software development environment Khoros 2.2 (Khoral Research, Albuquerque, NM).

Results

The main stages of automatic shape analysis are depicted in **Figure 6**. The cytologic sample (**Figure 6a**) is binarized to segment objects from background by local adaptive thresholding. At this stage, the segmentation results still include noise and unwanted smaller compartments (**Figure 6b**). Morphologic filtering yields

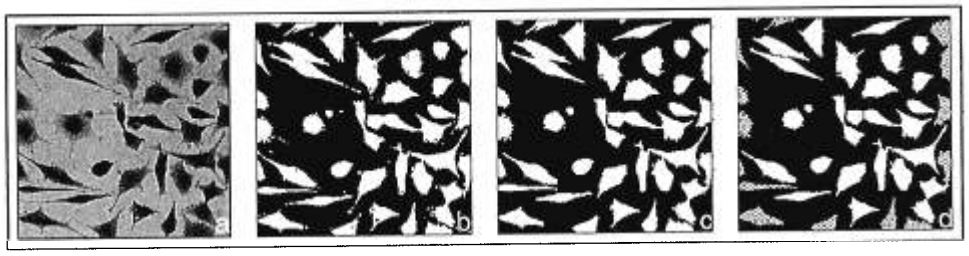

Figure 6. A micrograph of a cytological sample (microscopic magnification, ×100). After binarization (b), morphological filtering (c), and deagglomeration (d), the population of cells is separated. The striped objects touch the image border and therefore, they are dropped before quantification.

only those binary objects that correspond to cells (**Figure 6c**). The deagglomeration algorithm results in separated cells that are prepared for subsequent quantification (**Figure 6d**).

The central presupposition for automatic quantification of the morphologic changes is a segmentation and separation of highest possible quality. The example in **Figure 6d** contains only two minor differences from the separation that an expert would draw. Such separation quality enables robust quantification of shape deformations. To evaluate the quality of the automatic analysis, the manual cell segmentation and separation of an expert has to be compared with the results of the algorithm. Qualitatively the effects of the incubations with different concentrations can be described as follows:

The ethanol concentration was stable for 8 hours of incubation time. From 8 to 24 hours there was a decrease to approximately 67–73% of the initial concentration. Morphologic assessment of cytotoxic effects of ethanol seen with a light microscope gave a concentration dependent cell response. The incubation time of 24 hours was chosen in accordance with the ISO10993/EN30993 (part 5), which recommended an incubation time of 24 to 72 hours with the test medium. Ethanol was used as a positive control, which provides a reproducible cytotoxic response. Cytotoxic effects were detected after a short incubation time of 5 to 10 minutes of exposure to 15% ethanol using the trypan blue exclusion test and 3H-thymidine incorporation.[31] Without ethanol, the cells showed no visible signs of pathologic aberrations. Size and shape of nuclei and nucleoli were unaltered. The cytoplasm did not show any symptoms of vacuolization; only the mitotic cells were rounded up with the typical dumbbell-shape appearance. All other cells were well spread out and had the typical shape of murine fibroblasts. Ethanol (5%) in cell culture medium influenced mainly the cell number on the substrate, with cell density and number of mitotic cells clearly diminished. The cell shape was not altered dramatically. After incubation with 10% ethanol, the cells showed explicit pathologic attributes. Most cells were rounded up and the nuclei were compressed. No mitotic cells were visible and the cells lost the typical appearance of murine fibroblasts.

Because no morphologic differences were noticeable between the 10% incubated cells and higher concentrations, we neglected the quantitative assessment of ethanol concentrations higher than 10%. For the automated deformation analysis, 268 images were captured for each of the three concentrations of ethanol. This represents a total examination area of approximately 68.6 mm^2. The control parameters were experimentally determined to $n = 2$, $m = 4$, and $l = 12$.

The quantitative results are shown in **Figure 7**. Distributions of the compactness and a scatter plot of equally sized representative samples of the three concentrations of ethanol are given. As discriminative parameters of the distributions, the 25%, 50%, and 75% intervals are visualized. Additionally, the mean of the compactness distribution is given. The scatter diagrams show the relationship between size (*x*-axis) and perimeter (*y*-axis) of the cells in the samples. Cells that are perfectly circular would lay on the ideal circle line, which represents a lower limit for the plots. The grid shows the center of gravity of the set.

For quantitative analysis, a set of eight parameters was calculated to discriminate between the concentrations of ethanol: the three intervals and the mean of the compactness distribution, the center of gravity of the scatter plot, the density of the population, and the coverage of the cells (**Table 1**). All parameters, regardless of the coverage, require the separation of the agglomerated cells. Because density and coverage are dependent upon the number of cells in the population, they yield the best discrimination between the different concentrations. More objective quantifications of the actual shape are given by parameters that are independent of the number of cells because they represent only geometric features. These are the ones shown in **Figure 7**. Such more complex parameters are in general more robust because they incorporate different geometric properties of the cells instead of incorporating cell quantities.

The distribution- and scatter-diagrams show good discrimination between 10% and lower concentrations. The difference between 0% and 5% concentration is obvious in both diagrams. From 0% to 5%, the changes in compactness show a tendency toward toxic response, whereas the scatter plot shows good discrimination between the corresponding concentrations. Even better discrimination can be achieved by incorporating parameters such as density and coverage.

Because the compactnesses are obviously not normally distributed, a Wilcoxon two sample test was used to decide whether the distributions differ significantly. For all pairs of ethanol concentration, 0% (29,939 cells; mean compactness, 0.465; standard deviation, 0.200) and 5% (19,801 cells; mean compactness, 0.514; standard deviation, 0.236); 0% and 10% (10,495 cells; mean compactness, 0.711; standard deviation, 0.259); and 5% and 10%, the hypothesis of equal distributions can be rejected ($p < 0.0001$). Therefore, the compactness of cells is an appropriate indicator of toxicity. This result was also found for the additional parameters of density and coverage.

Discussion

To obtain reproducible and statistically expressive cytometric data, a large number of samples have to be acquired and analyzed. Computer-assisted microscopy can provide methods that increase quality and comparability of clinical studies by reducing the subjective influence of human operators on the results. To guarantee correctness of extracted parameters, reliable segmentation techniques are required. Expressive results are obtained if the extracted parameters discriminate between *a priori* defined and well known pathologic states. In the case of cytotoxicity evaluation of biomaterials via quantification of morphologic changes, the segmentation is performed by a special local adaptive thresholding technique. The actual separation of agglomerated cells is performed by a novel cascaded separation technique, based on mathematic morphology.

Table 1. Eight Selected Discriminative Parameters are Shown for the Three Tested Concentrations of Ethanol

	Concentration of ethanol		
	0%	5%	10%
25% interval	0.3	0.3	0.5
50% interval	0.42	0.46	0.8
75% interval	0.6	0.72	0.94
Mean compactness	0.465	0.514	0.711
Center of gravity—*x*	348.9	287.9	141.2
Center of gravity—*y*	101.8	90.0	53.0
Density (cells/mm^2)	422.9	279.7	38.0
Coverage (%)	16.07	8.92	2.55

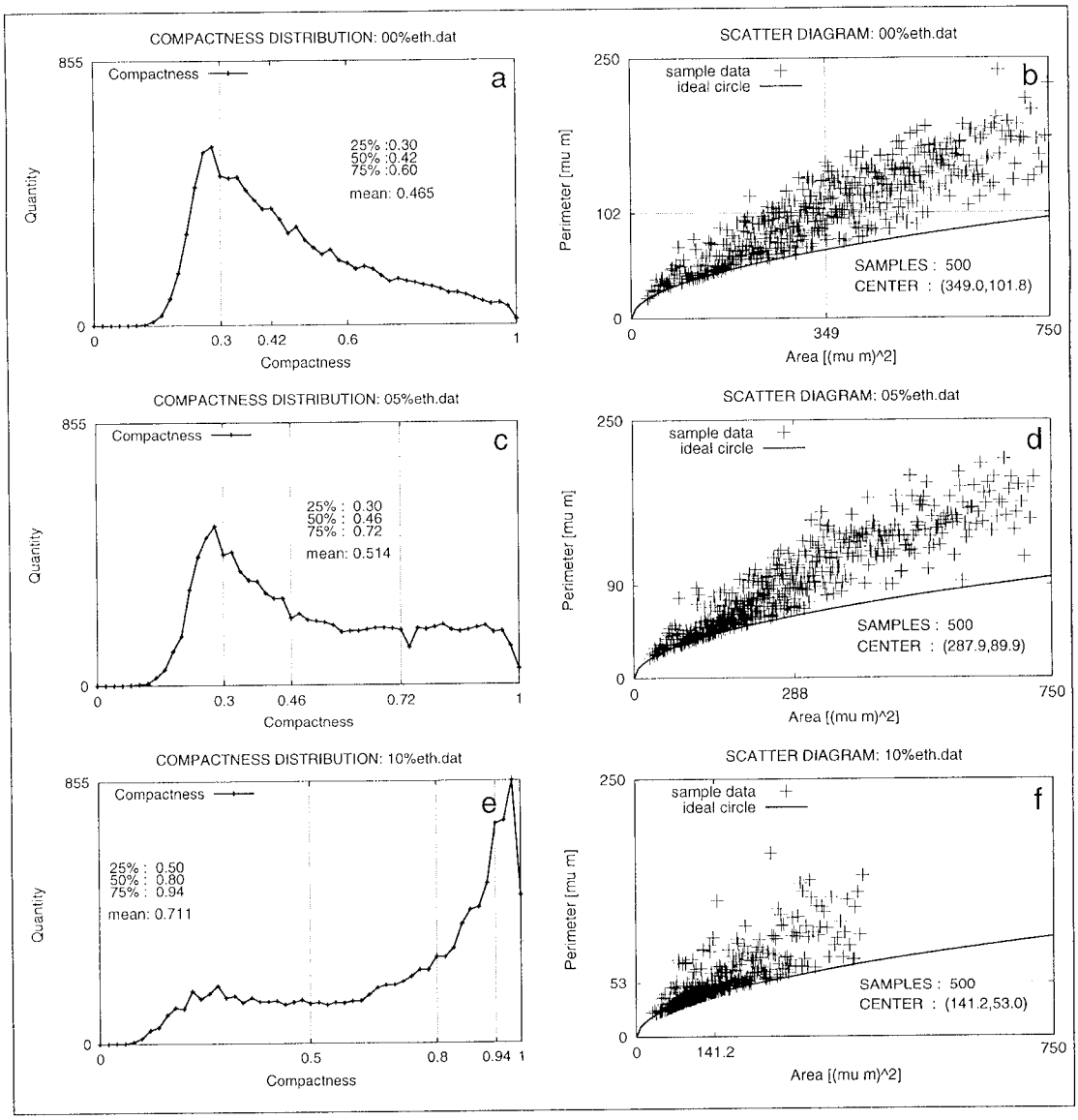

Figure 7. The diagrams show the results of cytotoxicity tests with L-929 fibroblasts and 0%, 5%, and 10% ethanol as toxin. In the left column, the distributions of compactness of representative samples of approximately 10,000 cells are shown. The 25%, 50% (median), and 75% intervals and the mean compactness are given as features of the distribution. The right column shows scatter diagrams for 500 representative cells, with the covered area on the *x*-axis and perimeter on the *y*-axis. The center of the scatter plots is marked by the grid.

The quantitative parameters extracted by the proposed method show good correlation with the qualitative evaluations of an expert. Hence, it is suitable for analyzing artificial organs with large surfaces such as dialysis membranes or oxygenators. In this case, the material has to be scanned uniformly before the homogeneity of the material can be analyzed. The method is extendable to cells with direct contact to the biomaterial, where dilution series are required to create appropriate dose/effect curves of the material. However, the analysis of large surfaces requires a mosaic function that puts together the single samples. The samples then have to be acquired with sufficient overlap to provide information for the spatial reconstruction of the entire population.

All presented parameters are determined automatically. One has to keep in mind that all data represents complex biologic features. Hence, the method of representing and visualizing the data is crucial to the discrimination of phenomena; this effect can be seen in **Figure 7**. The information yielded by the compactness distribution and the scatter plots are equal, because both sets contain information on the area and perimeter of the cells. Nevertheless, the scatter plots generally provide better discrimination between the toxic classes than the compactness distributions, because it is easier to recognize a qualitative difference between the ethanol concentrations in the scatter plots. This effect is independent of the center of gravity. Other quantitative parameters, like the main axis of the best fitting ellipsoid of the scatter plot or the number of second derivative zeros in cell shapes, reduce the information in the diagrams in **Figure 7**. They compress the information toward synthesized numeric values and may provide good discrimination between the toxic classes. The parameters are gathered as feature vectors that represent points in multidimensional space. Clustering methods determine thresholds that

show whether cells are pathologically changed by a biomaterial or not.

The usefulness and applicability of our method was demonstrated. Both qualitative and quantitative descriptions are appropriate to evaluate cytotoxic potentials of biomaterials. However, the automatic method cannot substitute for all microscopic assessments of cell cultures. Compared with the usual verbal description, the following advantages of the presented computer assisted shape analysis as part of a system for quantitative microscopy can be summarized:

The results are independent of subjective interpretations by human observers.

Cytotoxic influences of biomaterials can be standardized, which makes them comparable for interdisciplinary research.

Threshold values for the classification of biomaterials as toxic or nontoxic can be determined.

The method is especially suitable for the screening of a large number of material modifications, such as polymer blends and surface modifications.

They are appropriate to assess the response to negative and positive reference material. Validity of test results is only given if the results of the control sets lie within an expected range.

The automatization leads to a significant speed-up in preparing a study with negligible reduction of quality.

The presented algorithms can be adapted to all adherent cells obtained in monolayers. Presently, the method is under modification to adapt it to quantification of thrombocyte adhesion.

The relevance of the extracted quantitative parameters remains to be evaluated. The analysis of deformed L-929 cells incorporates the determination of dose/effect curves for ethanol. This is important because although we can provide different quantitative parameters, we do not yet know which of them is best for discrimination of toxic classes via dose/effect curves. One demand on suitable parameters is their independence of the number of cells acquired, because coverage and density of a population (**Table 1**) may yield different values for the ethanol concentrations but cannot be used to create dose/effect curves. Once dose/effect curves exist and determine the range of the main parameters, quality control of future tests is possible via the positive and negative references.

In further studies we will use extracts of recommended negative and positive control materials, such as high density polyethylene and organo-tin poly(vinylchloride). The sensitivity of the method will be evaluated by comparison with other established test systems including the XTT-test (tetrazolium salt) and proliferation test.

Acknowledgment

This work was done in the framework of the Interdisciplinary Center of Research on Biomaterials (IZKF "*BIO*MAT"), Aachen University of Technology (RWTH), Germany. The funding of the Federal Ministry of Education, Science, Research, and Technology (BMBF Grant No. 01ks9503/9) is gratefully acknowledged.

References

1. Gurland HJ, Davison AM, Bonomini V, *et al*: Definitions and terminology in biocompatibility. *Nephrol Dial Transplant* 9(Suppl 2): 4–10, 1994.
2. Doillon CJ, Cameron K: New approaches for biocompatibility testing using cell culture. *Int J Artif Organs* 13: 517–520, 1990.
3. Smith MD, Barbenel JC, Courtney JM, Grant MH: Novel quantitative methods for the determination of biomaterial cytotoxicity. *Int J Artif Organs* 15: 191–194, 1992.
4. Biologische Beurteilung von Medizinprodukten, Teil 5: Prüfung auf Zytotoxzität: in vitro Methoden. *Ref Nr DIN EN* 30993-5: 1994–2008.
5. Tapani E, Taavitsainen M, Lindros K, Vehmas T, Lehtonen E: Toxicity of ethanol in low concentrations. Experimental evaluation in cell culture. *Acta Radiol* 37: 923–926, 1996.
6. Laev H, Hungund BL, Karpiak SE: Cortical cell plasma membrane alterations after in vitro alcohol exposure: prevention by GM1 ganglioside. *Alcohol* 13: 187–194, 1996.
7. Chen SY, Yang B, Jacobson K, Sulik KK: The membrane disordering effect of ethanol on neural crest cells in vitro and the protective role of GM1 ganglioside. *Alcohol* 13: 589–595, 1996.
8. Higashi K, Hoshino M, Nomura T, Saso K, Ito M, Hoek JB: Interaction of protein phosphatases and ethanol on phospholipase C-mediated intracellular signal transduction processes in rat hepatocytes: role of protein kinase A. *Alcohol Clin Exp Res* 20:320A–324A, 1996.
9. Klein RF, Fausti KA, Carlos AS: Ethanol inhibits human osteoblastic cell proliferation. *Alcohol Clin Exp Res* 20: 572–578, 1996.
10. Ni Y, Feng-Chen KC, Hsu L: A tissue culture model for studying ethanol toxicity on embryonic heart cells. *Cell Biol Toxicol* 8: 1–11, 1992.
11. Beumer GJ, van Blitterswijk CA, Bakker D, Ponec M: Cell-seeding and in vitro biocompatibility evaluation of polymeric matrices of PEO/PBT copolymers and PLLA. *Biomaterials* 14: 598–604, 1993.
12. Ciapetti G, Roda P, Landi L, Facchini A, Pizzoferrato A: In vitro methods to evaluate metal-cell interactions. *Int J Artif Organs* 15: 62–66, 1992.
13. Young IT: Quantitative microscopy. *IEEE Engineer Med Biol* 15: 59–66, 1996.
14. Dougherty ER: *An introduction to Morphological Image Processing*. Bellingham, WA: SPIE Optical Engineering Press, 1992.
15. Pei S-C, Lai C-L: An efficient class of alternating sequential filters in morphology. *Graphic Models Image Proc* 59: 109–116, 1997.
16. Meyer F, Beucher S: Morphological segmentation. *J Visual Commun Image Represent* 1: 21–46, 1990.
17. Godbole S, Amin A: Mathematical morphology for edge and overlap detection for medical images. *Real Time Imaging* 1: 191–201, 1995.
18. MacAulay C, Palcic B: A comparison of some quick and simple threshold selection methods for stained cells. *Analyt Quantitat Cytol Histol* 10: 134–138, 1988.
19. Leung CK, Lam FK: Performance analysis for a class of iterative image thresholding algorithms. *Pattern Recognition* 29: 1523–1530, 1996.
20. Murray C, O'Malley M: Segmentation of plant cell pictures. *Image Vision Comput* 11: 155–162, 1993.
21. Kovalev VA, Grigoriev AY, Ahn H-S, Myshkin NK: Automatic localization and feature extraction of white blood cells. In: *SPIE Proceedings*, Bellingham, WA, Vol. 2434, 1996, pp. 754–765.
22. Otsu N: A threshold selection method from grey level histograms. *IEEE Trans Syst Man Cybernet* 9: 62–66, 1979.
23. Serra J: *Image Analysis and Mathematical Morphology*. London, Academic Press, 1982.
24. Borgefors G: Distance transforms in digital images. *Comput Vision Graph Image Process* 34: 679–698, 1986.
25. Russ JC: *Computer-Assisted Microscopy*. New York, Plenum Press, 1990.
26. Glasbey CA, Horgan GW: *Image Analysis for the Biological Sciences*. Chichester, UK: Wiley & Sons, 1995.
27. Payne CM, Bjorne Jr. CG, Cromey DW, Roland F: A comparative mathematical evaluation of contour irregularity using form factor and PERBAS, a new analytic shape factor. *Analyt Quantitat Cytol Histol* 11: 341–352, 1989.